Soil Moisture Estimation Using Landsat-8 Satellite Data: A Case Study the Karshi Steppe, Uzbekistan

Sichugova, L.* and Fazilova, D.
Astronomical Institute of Uzbek Academy of Science, 100052, Astronomicheskaya 33, Tashkent, Uzbekistan,
E-mail: dil_faz@yahoo.com, slola988@gmail.com*
Corresponding Author

DOI: https://doi.org/10.52939/ijg.v18i1.2109

Abstract

This study presents the results of soil moisture estimation using Landsat-8 for the Karshi Steppe territory (Uzbekistan). Soil moisture estimation was carried out using the soil moisture index (SMI) calculated based on surface temperature (LST) and the normalized difference vegetation index (NDVI). Thermal Infrared Sensor (TIRS) and Red, Near-Infrared (NIR) bands of Landsat-8 were used to calculate LST and NDVI. Observation shows that NDVI and LST are considered essential data to obtain SMI calculation. The study made it possible to categorized 4 class results of SMI from very wet to very dry of the soil edge. The final result is obtainable with the values range from 0 to 1. The results indicate that this method from Landsat images is valuable for monitoring agricultural drought and flood disaster assessment. It is shown that the method can efficiently be applied to estimate soil moisture using remote sensing, which has some advantages over traditional methods and can be effectively used to monitoring soil moisture in agricultural areas of the Karshi Steppe.

1. Introduction

Soil moisture is a dimensionless quantity that characterizes the moisture content in the soil. Numerous studies (Choi et al., 2011 and Berg et al., 2014) have shown that soil moisture affects the interaction between the Earth's surface and the atmosphere. Soil moisture is the level of saturation in the upper soil layer relative to the soil field capacity. Soil moisture depends on precipitation, potential evaporation, temperature, soil characteristics (Eltahir Elfatih, 1998). Soil moisture plays an important role in many environmental phenomena include agricultural and hydrological applications (Ahmad et al., 2011 and Lakshmi, 2013).

Many soil moisture datasets have been produced from various spaceborne instruments using different algorithms (Owe et al., 2001, Njoku et al., 2003 and Naeimi et al., 2009). Some of these datasets, obtained from both active and passive microwave remote sensing, have been combined (Liu et al., 2011) to form a global soil moisture dataset. In (Srivastava et al., 1997) the method for assessing soil moisture content, depending on the amount of electromagnetic energy reflected and radiated from the Earth's surface. The amount of water is determined using the maximum and minimum values of the thermal and daily soil properties. They are measured in the thermal infrared and microwave ranges. The active and passive microwave takes into account the measurement of the radar backscatter coefficient and the brightness temperature, respectively.

There are many studies on estimating soil moisture using both passive (Sadeghi et al., 2017), and active remote sensing satellites (Srivastava et al., 2009, Şekertekin et al., 2016). Passive methods retrieve soil moisture information independently even when there is a vegetation canopy available and it provides information about land properties, such as surface temperature and Normalized Difference Vegetation Index (NDVI). Passive methods provide Land Surface Temperature (LST) and Normalized Difference Vegetation Index (NDVI) information regardless of the presence of vegetation cover. Studies confirm that there is a correlation of about 95% between soil moisture with the LST and NDVI (Entezari et al., 2019). In the paper (Trinh et al., 2018) presented the estimation of soil moisture was carried out using the temperature-vegetation index (TVDI), calculated based on the surface brightness temperature and NDVI.

This study presents the results of soil moisture estimation using Landsat-8 for the part of the Karshi Steppe territory (Kashkadarya, Uzbekistan) (Figure 1).

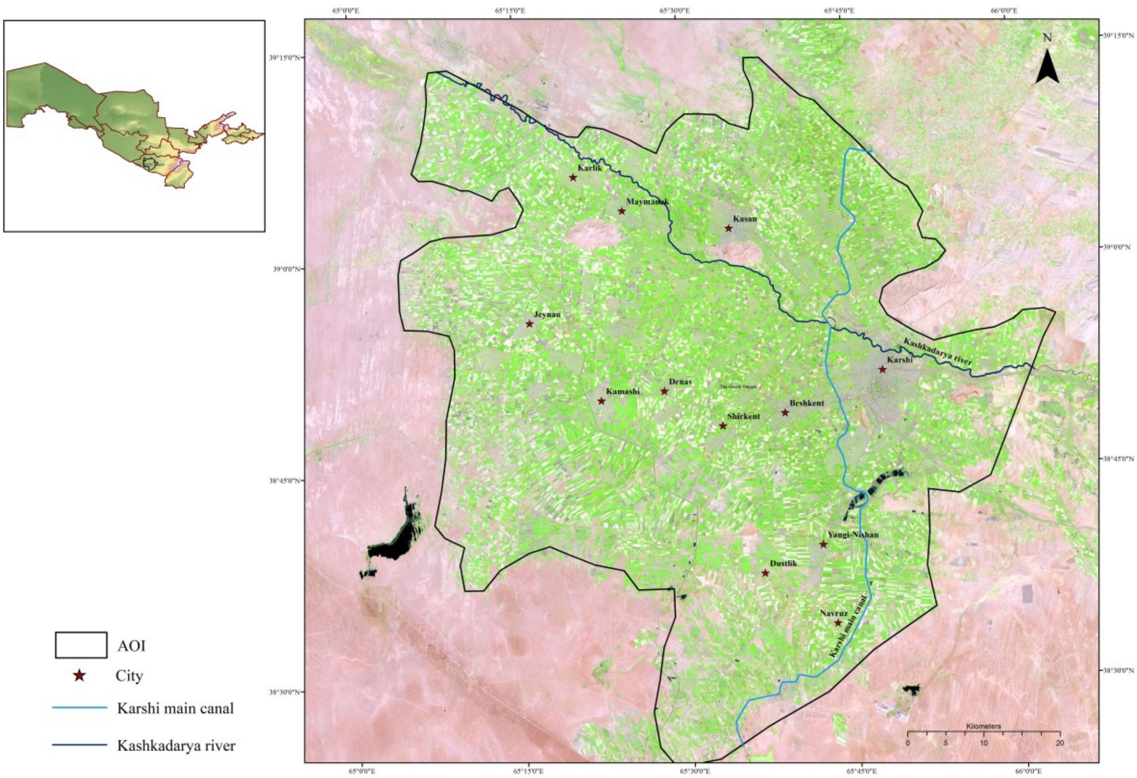

Figure 1: Location the part of the study area Karshi Steppe, Kashkadarya, southern Uzbekistan

2. Study Area

The Karshi Steppe is plain in Uzbekistan, located at the west of the Zeravshan and Gissar ranges. The Steppe is covered with river deposits of constant water flows. The waters of the Kashkadarya River and the Karshi main canal are irrigating the Steppe. The climate of the region is arid; the amount of precipitation is 200-400 mm per year. The soil cover of the steppe is varied. Typical and light serosem are widely developed. Soils of the Karshi Steppe are subdivided into intact and altered soils during irrigation, and also soils differ by texture and degree of salinization. A significant part of the land in the Karshi Steppe is used for cereal crops and cotton (Chembarisov et al., 2015). The population is engaged in agriculture. The limiting factor for its further development is water since the flow of rivers flowing into the steppe is almost entirely spent on irrigation. That is why it is necessary, firstly, from time to time to revise the information on water resources based on the latest hydrological information, and secondly, further for methods to develop soil moisture estimation.

3. Data and Method

For this study were used images of the Landsat-8 images with 30 m resolution from the United States Geological Survey (USGS) Earth Explorer website were obtained for June, July, August, and September 2020. Cloud-free images were used. In this study were used Red and Near-Infrared (NIR) for the NDVI calculation and thermal infrared (TIR) bands for the LST calculation. One method for estimating soil moisture is called the triangle method. The triangle method is based on the empirical relationship between soil moisture, surface temperature, and vegetation cover. The triangle method was used in several studies to estimate soil moisture, notably Carlson et al., (1994) and Sandholt et al., (2002). The method considers the interrelation of temperature with vegetation, based on which the soil moisture is estimated. The maximum dry edge of the soil is equal to 1, and the minimum wet edge equals 0. The soil moisture index is based on the relationship between LST and NDVI. In the first step, we have to convert Digital Number (DN) to the Top of Atmosphere (TOA) spectral radiance to used equation (1) (Landsat 8 (L8) Data Users Handbook, 2019).

$$L_\lambda = M_\lambda Q_{cal} + A_\lambda$$

Equation 1

Where L_λ is TOA spectral radiance (Watts/ (m^2*srad*µm)), M_L is band-specific multiplicative

ISSN 2673-0014 (Online) / © Geoinformatics International

rescaling factor from metadata, A_L is band-specific additive rescaling factor from the metadata, Q_{cal} is quantized and calibrated standard product pixel values (Digital Number). Now we are calculating Brightness Temperature using the thermal constant (Landsat 8 (L8) Data Users Handbook, 2019):

$$T = \frac{K_2}{\ln\left(\frac{K_1}{L_\lambda}+1\right)} - 273.15$$

Equation 2

Where T is the top of atmosphere brightness temperature (K), L_λ is TOA spectral radiance (Watts/ (m^2*srad*μm)), K_1, K_2 are bands-specific thermal conversion constant from the metadata. And finally step is calculating LST (Jeevalakshmi et al., 2017):

$$LST = \frac{T}{1+\frac{\lambda T}{\rho}\ln\varepsilon}$$

Equation 3

Where T is the top of atmosphere brightness temperature, λ is the wavelength of emitted radiance, ρ is constant (1.438*10^{-2} m K), ε is the emissivity. In (Valor and Caselles, 1996) the emissivity ε is determined based on the NDVI and can be applied to heterogeneous areas and various types of surfaces:

$$\varepsilon = \varepsilon_v P_v + \varepsilon_S(1-P_v)$$

Equation 4

Where ε_v, ε_s is the emissivity of the vegetation and soil, P_v is the value of the vegetation in a specific pixel.
Here P_v can be determined using values of the NDVI:

$$NDVI = \frac{NIR - RED}{NIR + RED}$$

Equation 5

$$P_v = \left(\frac{NDVI - NDVI_{\min}}{NDVI_{\max} - NDVI_{\min}}\right)^2$$

Equation 6

Where NIR is the reflectance values of the Near Infrared band, RED is the reflectance values of the Red band, $NDVI_{min,\,max}$ represents the maximum and minimum value of the NDVI pixel.

NDVI values range from –1 to 1. High photosynthetic activity leads to lower reflectance in the red region of the spectrum and higher values in the near infrared. The ratio of these indicators to each other makes it possible to clearly distinguish vegetation from other natural objects. The index only takes positive values. NDVI values cannot be less than 0 for vegetation. And the final step is calculating SMI:

$$SMI = \left(\frac{LST_{\max} - LST}{LST_{\max} - LST_{\min}}\right)$$

Equation 7

Where $LST_{max,\,min}$ represents the maximum and minimum surface temperature.

4. Results and Discussion

The results of the LST calculations are shown in Figure 2 (a), (b), (c) and (d). The LST values are measured in °C. As a result of the analysis of the results obtained, it was noted that an area with a high surface temperature belongs to bare agriculture fields. The difference between the maximum and minimum surface temperatures for June 2020 was 38.83°C (Figure 2(a)). This difference was the largest among other observations. The difference LST values for July 2020, August 2020, and September 2020 was 26.31°C (Figure 2(b)), 23.87°C (Figure 2(c)), 29.45°C (Figure 2(d)) respectively. SMI was determined after calculating the LST and NDVI (Figure 3 (a), (b), (c) and (d). The calculation of the SMI made it possible to identify the edge for the territory of the soil, which represents aridity and moisture (Table 1). SMI values range from 0 to 1. Identified 4 categories: Very dry – 0-0.2; Dry – 0.2-0.3; Wet – 0.3-0.5; Very wet – 0.5-1.

Table 2 present analyzes soil moisture areas per category for different periods in ha. Results show, that the amount of “Very wet” in June was 16907.53 ha (Figure 3(a)). But here, some part of the territory is covered by clouds (23.11% from the metadata file). Most of the territory belongs to the category “Dry” the amount was 191314.82 ha in June. Almost whole the territory “Very dry” belongs to bare fields. The maximum amount of “Very dry” lands was in June (127588.86 ha). In contrast, July, August, and September are periods with fewer area “Very dry” fields. We observed that “Very wet” fields are increasing in July (Figure 3(b)). It is a result of the irrigation works. We observed that amount of “Wet” and “Very wet” was higher at 167203.63 ha and 118497.01 ha respectively in September in contrast with other periods (Figure 3(c)). The entire category of “Very dry” belongs to bare fields.

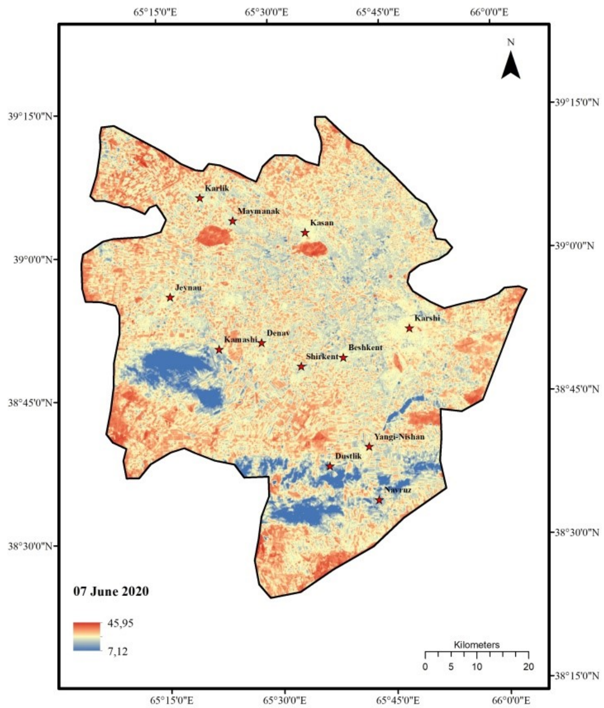

a) June 07, 2020

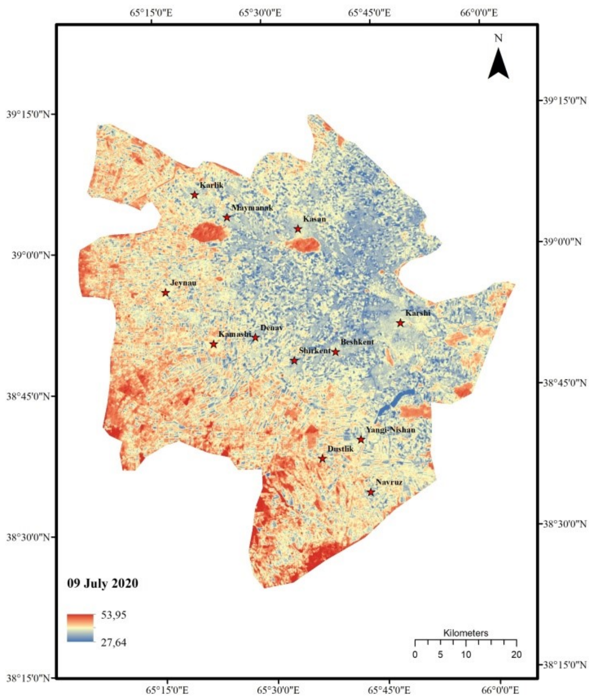

b) July 09, 2020

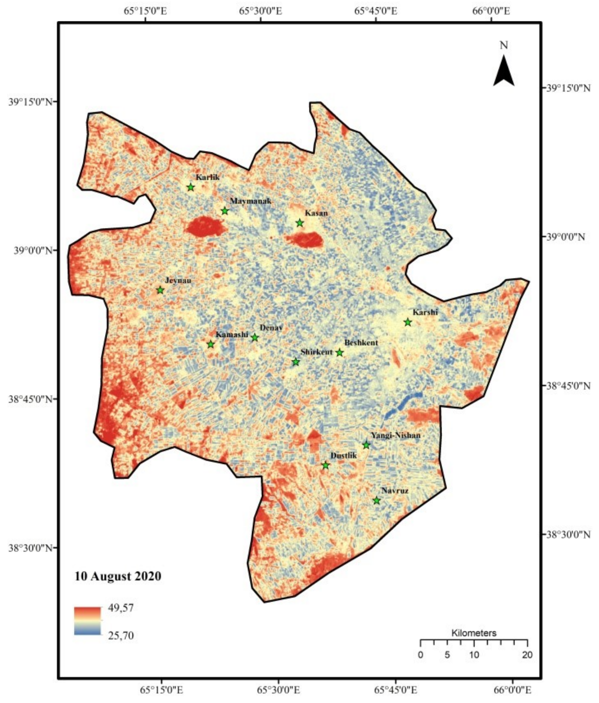

c) August 10, 2020

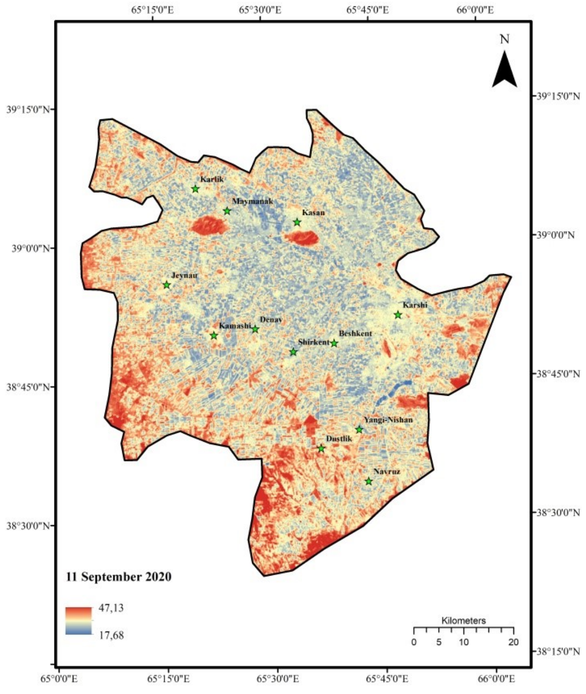

d) September 11, 2020

Figure 2: LST maps

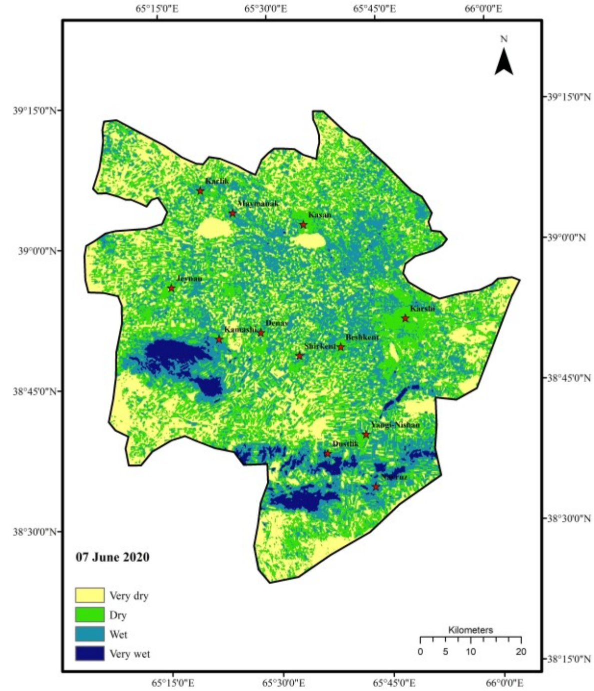

a) June 07, 2020

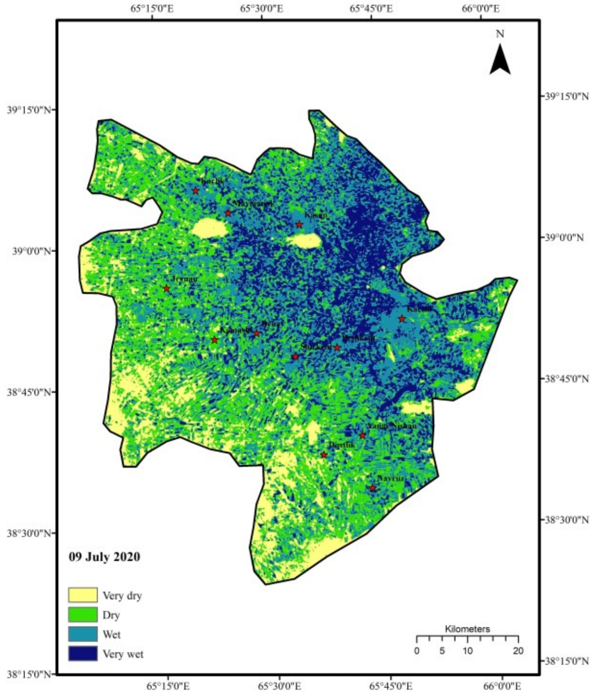

b) July 09, 2020

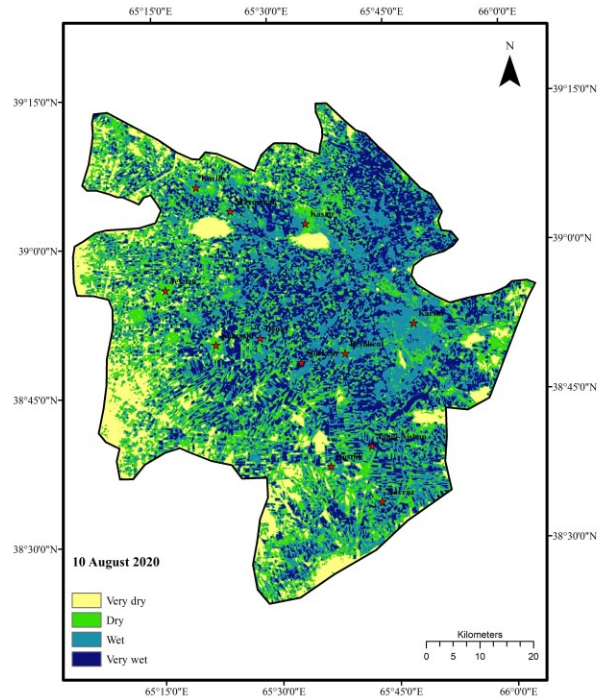

c) August 10, 2020

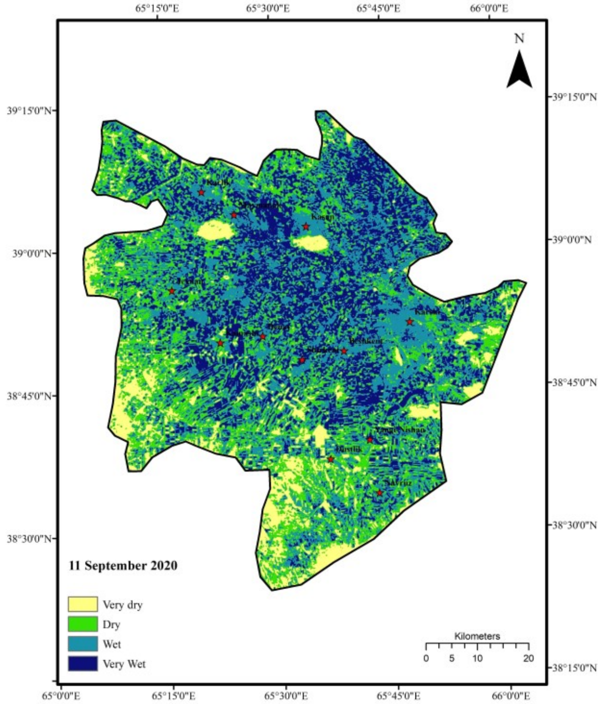

d) September 11, 2020

Figure 3: SMI maps

Table 1: Soil classification based on SMI

№	SMI value	Classification
1	0 – 0.2	Very dry
2	0.2 – 0.3	Dry
3	0.3 – 0.5	Wet
4	0.5 – 1	Very wet

Table 2: Area of the soil moisture

Classification	June	July	August	September
Very dry	127588.86	62991.36	62123.10	51995.60
Dry	191314.82	147310.07	121139.68	121457.46
Wet	123350.97	160831.42	166609.27	167203.63
Very wet	16907.53	88823.40	109280.20	118497.01

5. Conclusion

In this work, we have estimated soil moisture using LST and SMI. The results show that the SMI can be used according to the triangle method for soil moisture estimation in the Karshi Steppe. Information obtained in results used satellites images allows getting information about the condition of the water balance in agriculture and bare fields. In results of LST was noted that an area with a high surface temperature belongs to bare agriculture fields. The calculation of the SMI made it possible to identify the edge for the territory. SMI values range from 0 to 1. Identified 4 categories: Very dry – 0-0.2; Dry – 0.2-0.3; Wet – 0.3-0.5; Very wet – 0.5-1. We observed that "Very wet" fields are increasing from July. It is a result of the irrigation works. The area of "Wet" and "Very wet" was higher at 167203.63 ha and 118497.01 ha respectively in September in contrast with other periods. Results show that the maximum amount of "Very dry" fields in June (127588.86 ha). In contrast, July, August, and September are periods with less area of "Very dry" fields.

We can conclude that optical remote sensing is still an effective technique for estimating soil moisture, due to reflected solar radiation is the strongest passive signal available to satellites, and therefore observations at optical wavelengths can provide data with high spatial resolution. LST and NDVI are two important parameters that indicate the conditions of soil moisture. The processing technique in this study can be used for operational mapping of soil moisture to plan mitigating measures for the effects of drought and desertification on the environment.

References

Ahmad, A., Zhang, Y. and Nichols, S., 2011, Review and Evaluation of Remote Sensing Methods for Soil-Moisture Estimation. *SPIE 028001. Reviews*, Vol. 2(1). http://doi.org/10.1117/1.3534910.

Berg, A., Lintner, B. R., Findell, K. L., Malyshev, S., Loikith, P. C. and Gentine, P., 2014, Impact of Soil Moisture–Atmosphere Interactions on Surface Temperature Distribution. *Journal of Climate*, Vol. 27, 7976-7993.

Carlson, T. N., Gillies, R. R. and Perry, E. M., 1994, A Method to Make Use of Thermal Infrared Temperature and NDVI Measurements to Infer Surface Soil Water Content and Fractional Vegetation Cover. *Remote Sensing Reviews*, Vol. 9, 161–173.

Chembarisov, E. I., Lesnik, T. Yu., Nasrulin, A. B. and Ergashev, A., 2015, Meliorative State of Lands and Formation of Collector-Drainage Water on Irrigated Lands of Kashkadarya Region of the Republic of Uzbekistan. *Puti povisheniya Effectivnosti Oroshaemogo Zemledeliya (Conference)*, Vol. (57), 95-99.

Choi, M., Woong K. T. and Kustas, W. P., 2011, Reliable Estimation of Evapotranspiration on Agricultural Fields Predicted by the Priestley–Taylor Model Using Soil Moisture Data from Ground and Remote Sensing Observations Compared with the Common Land Model. *International Journal of Remote Sensing*, Vol. 32(16), 4571–4587. https://doi.org/10.1080/01-431161.2010.489065.

Eltahir Elfatih A. B., 1998, A Soil Moisture-Rainfall Feedback Mechanism. 1. Theory and Observations. *Water Resources Research*, Vol. 34(4), 765-776.

Entezari, M., Esmaeily, A. and Niazmardi, S., 2019, Estimation of Soil Moisture and Earth's Surface Temperature Using Landsat-8 Satellite Data. *The International Archives of the Photogrammetry, Remote Sensing and Spatial Information Sciences*, Volume XLII-4/W18, 327-330, DOI:10.5194/isprs-archives-XLII-4-W18-327-2019.

Jeevalakshmi, D., Narayana Reddy, S. and Manikiam, B., 2017, Land Surface Temperature Retrieval from LANDSAT Data Using Emissivity Estimation. *International Journal of Applied Engineering Research*, Vol. 12, 9679-9687.

Lakshmi, V., 2013, Remote Sensing of Soil Moisture. *ISRN Soil Science*, 1–33. http://doi.org/10.1155/2013/424178.

Landsat 8 (L8) Data Users Handbook, 2019, Version 5.0, EROS, Sioux Falls, South Dakota, 1- 106.

Liu, Y. Y., Parinussa, R. M., Dorigo, W. A., De Jeu, R. A. M., Wagner, W., A. I. J. M van Dijk, McCabe M. F. and Evans, J. P., 2011, Developing an Improved Soil Moisture Dataset by Blending Passive and Active Microwave Satellite-Based Retrievals. *Hydrology and Earth System Sciences*, Vol. 15, 425–436.

Naeimi, V., Scipal, K., Bartalis, Z., Hasenauer, S. and Wagner, W., 2009, An Improved Soil Moisture Retrieval Algorithm for ERS and MetOp Scatterometer Observations. *IEEE Transactions on Geoscience and Remote Sensing*, Vol. 47(7), 1999-2013.

Njoku, E. G., Jackson, T. J., Lakshmi, V., Chan, T. K. and Nghiem, S. V., 2003, Soil Moisture Retrieval from AMSR-E. *IEEE Transactions on Geoscience and Remote Sensing*, Vol. 41(2), 215–229.

Owe, M., de Jeu, R. and Walker, J., 2001, A Methodology for Surface Soil Moisture and Vegetation Optical Depth Retrieval Using the Microwave Polarization Difference Index. *IEEE Transactions on Geoscience and Remote Sensing*, Vol. 39(8), 1643–1654. DOI:10.1109/36.942542.

Sadeghi, M., Babaeian, E., Tuller, M and Jones, S. B., 2017, The Optical Trapezoid Model: A Novel Approach to Remote Sensing of Soil Moisture Applied to Sentinel-2 and Landsat-8 Observations. *Remote Sensing of Environment*, Vol. 198, 52–68. http://doi.org/10.1016/j.rse.2017.05.04.

Sandholt, I., Rasmussen, K. and Andersen, J., 2002, A Simple Interpretation of the Surface Temperature/Vegetation Index Space for Assessment of Surface Moisture Status. *Remote Sensing of Environment*, Vol. 79(2–3), 213–224.

Sekertekin, A., Marangoz A. M. and Abdikan, S., 2016, Soil Moisture Mapping Using Sentinel-1A Synthetic Aperture Radar Data. *IJEGEO*, Vol. 5(2), 178-188.

Srivastava, S. K., Yograjan, N., Jayaraman, V., Nageswara Rao, P. P. and Chandrasekhar, M. G., 1997, On the Relationship between ERS-1 SAR/Backscatter and Surface/Sub-surface Soil Moisture Variations in Vertisols. *Acta Astronautica*, Vol. 40(10), 693-699.

Srivastava, H. S., Patel, P., Sharma, Y. and Navalgund, R. R., 2009, Large-Area Soil Moisture Estimation Using Multi-Incidence-Angle RADARSAT-1 SAR Data. *IEEE Transactions on Geoscience and Remote Sensing*, Vol. 47(8), 2528–2535. http://doi.org/10.1109/TGRS.2009.2018448.

Trinh, L. H., Zablotskii, V. R. and Dao, K. H., 2018, A Study of the Long-Term Dynamics of Soil Moisture in the Bac Binh District (Binh Thuan province, Vietnam) Using Landsat Multispectral Images, Sovremennie Problem DZZ iz Kosmosa, Vol. 15 (7), 89-101. DOI: 10.21046/2070-7401-2018-15-7-89-101.

Valor, E. and Caselles, V., 1996, Mapping Land Surface Emissivity from NDVI: Application to European, African, and South American areas. *Remote Sensing of Environment*, Vol. 57, 167-184.